JACC: CARDIOVASCULAR IMAGING VOL. 6, NO. 4, 2013

ISSN 1936-878X/$36.00
PUBLISHED BY ELSEVIER INC. http://dx.doi.org/10.1016/j.jcmg.2012.09.016

Napkin-Ring Sign on Coronary CT Angiography for the Prediction of Acute Coronary Syndrome

Kenichiro Otsuka, MD,* Shota Fukuda, MD,† Atsushi Tanaka, MD,‡ Koki Nakanishi, MD,* Haruyuki Taguchi, MD,† Junichi Yoshikawa, MD,§ Kenei Shimada, MD,* Minoru Yoshiyama, MD*

Osaka, Tanabe, and Nishinomiya, Japan

OBJECTIVES The aim of this study was to determine the predictive value of the napkin-ring sign on coronary computed tomography angiography (CTA) for future acute coronary syndrome (ACS) events in patients with coronary artery disease.

BACKGROUND Recent studies have reported a close association between the napkin-ring sign on coronary CTA and thin-cap fibroatheroma.

METHODS The subjects of this prospective study were 895 consecutive patients who underwent coronary CTA examination and were followed for >1 year. The primary endpoint was an ACS event (cardiac death, nonfatal myocardial infarction, or unstable angina pectoris). The coronary CTA analysis included the presence of obstructive plaque, positive remodeling (PR), low-attenuation plaque (LAP), and the napkin-ring sign. The napkin-ring sign was defined by the following criteria: 1) the presence of a ring of high attenuation around certain coronary artery plaques; and 2) attenuation of the ring presenting higher than those of the adjacent plaque and no >130 Hounsfield units.

RESULTS Of the 12,727 segments, 1,174 plaques were observed, including plaques with PR in 130 segments (1.0%), LAP in 107 segments (0.8%), and napkin-ring signs in 45 segments (0.4%). Thirty-six of the 45 plaques with napkin-ring signs (80%) overlapped with those showing either PR or LAP. During the follow-up period (2.3 ± 0.8 years), 24 patients (2.6%) experienced ACS events, and plaques developed in 41% with a napkin-ring sign. Segment-based Cox proportional hazards models analysis showed that PR ($p < 0.001$), LAP ($p = 0.007$), and the napkin-ring sign ($p < 0.0001$) were independent predictive factors for future ACS events. Kaplan-Meier analysis demonstrated that plaques with napkin-ring signs showed a higher risk of ACS events compared with those without a napkin-ring sign.

CONCLUSIONS The present study demonstrated for the first time that the napkin-ring sign demonstrated on coronary CTA was strongly associated with future ACS events, independent of other high-risk coronary CTA features. Detection of the napkin-ring sign could help identify coronary artery disease patients at high risk of future ACS events. (J Am Coll Cardiol Img 2013;6:448–57) © 2013 by the American College of Cardiology Foundation

From the *Department of Internal Medicine and Cardiology, Osaka City University Graduate School of Medicine, Osaka, Japan; †Department of Medicine, Osaka Ekisaikai Hospital, Osaka, Japan; ‡Department of Cardiovascular Medicine, Social Insurance Kinan Hospital, Tanabe, Japan; and the §Nishinomiya Watanabe Cardiovascular Center, Nishinomiya, Japan. All authors have reported that they have no relationships relevant to the contents of this paper to disclose.

Manuscript received April 30, 2012; revised manuscript received August 13, 2012, accepted September 27, 2012.

The culprit plaques associated with acute coronary syndrome (ACS) contain large necrotic cores covered by thin fibrous caps (thin-cap fibroatheroma [TCFA]) and positive arterial remodeling (1–4). Coronary computed tomography angiography (CTA) is a developing imaging modality that permits the visualization of coronary atherosclerotic lesions, such as coronary artery stenosis (5–9), as well as plaque characteristics (10–15). Recent coronary CTA investigations showed that TCFA is described as a napkin-ring sign, coronary CTA-specific attenuation pattern of high-risk atherosclerotic plaques (16–21). However, the prognostic value of this feature has not been examined. In this prospective study, we investigated the relationship between the presence of a napkin-ring sign on coronary CTA and future ACS events in patients with coronary artery disease (CAD). We hypothesized that the napkin-ring sign is associated with future ACS events.

METHODS

Study population. This study included 960 consecutive patients scheduled to undergo coronary CTA for the evaluation of CAD between March 2007 and January 2010, 579 (60%) of whom were referred for coronary CTA examination because of chest pain of varying degrees and types. The remaining 381 patients (40%) were asymptomatic but referred for evaluation based on multiple CAD risk factors, including peripheral arterial disease, cerebrovascular disease, and abnormal findings on exercise-stress echocardiography or single-photon emission computed tomography. The exclusion criteria were as follows: 1) history of coronary artery bypass grafting; 2) valvular heart disease of more than moderate severity; and 3) chronic kidney disease. After coronary CTA examination, 65 patients were excluded due to severe coronary calcifications (n = 43) and atrial fibrillation (n = 22). The final study population comprised 895 patients (590 men; mean age 66 ± 10 years). Segments scheduled for revascularization within 1 month and those with previous revascularization were excluded from segmental analysis. These patients were included in the patient-based analysis. Blood samples were taken at the coronary CTA examination for measuring levels of serum creatinine, fasting lipids, glucose, glycated hemoglobin, and C-reactive protein. All patients were followed for >1 year by structured interviews by an attending physician. Patients were divided into groups based on whether ACS events occurred. This study was approved by the institutional review board of Osaka Ekisaikai Hospital, and the subjects gave their informed consent.

Scan protocol and image reconstruction. Coronary CTA was performed using a SOMATOM Sensation 64 system (Siemens Medical Systems, Forchheim, Germany), with the following scan parameters: 64 × 0.6-mm collimation, 120-kV tube voltage, gantry rotation time of 330 ms, and tube current rotation time of 770 to 850 mA. For the contrast-enhanced scans, 50 to 80 ml of nonionic contrast agent (Omnipaque 350, Daiichi Sankyo Co., Tokyo, Japan) was injected intravenously at a flow rate of 3.5 to 5.5 ml/s followed by 30 ml of saline. The delay time was determined using the bolus tracking technique with a region of interest positioned at the level of the ascending aorta in the monitoring scan and using a manually triggered threshold of 100 Hounsfield units (HU) for the main scanning. All patients took 5 mg bisoprolol orally before the scan, and patients with a heart rate >70 beats/min additionally received 2 mg metoprolol intravenously. All patients also received 0.6 mg of sublingual nitroglycerin. All scans were performed during a single breath-hold. The raw data were reconstructed using algorithms optimized for electrocardiography-gated multislice spiral reconstruction. Retrospective gating was used for all patients in this study because the coronary CTA research database was initially designed to assess coronary artery atherosclerosis, cardiac chamber volumes, and their function. The estimated radiation dose was 9 mSv.

ABBREVIATIONS AND ACRONYMS

ACS = acute coronary syndrome
CAD = coronary artery disease
CTA = computed tomography angiography
LAP = low-attenuation plaque
PR = positive remodeling
TCFA = thin-cap fibroatheroma

Analysis of coronary CTA. All coronary CTA datasets were analyzed by 2 experienced readers both with >5 years of experience in coronary CTA with the number of previous examinations performed equivalent to American College of Cardiology Foundation/American Heart Association clinical competence statement training level 3 (22). Coronary arteries were divided into 15 separate segments that were ≥1.5 mm in diameter as measured on the coronary CTA, according to the modified American Heart Association classification (23). In each coronary artery segment, coronary atherosclerotic plaque was defined as tissue structures >1 mm^2 that existed either within or adjacent to the coronary artery lumen and that could be discriminated from surrounding pericardial tissue, epicardial fat, and the vessel lumen itself (10). Coronary atheroscle-

JACC: CARDIOVASCULAR IMAGING, VOL. 6, NO. 4, 2013
APRIL 2013:448–57

rotic lesions were quantified for stenosis by visual estimation. The severity of luminal-diameter stenosis was divided into nonobstructive plaques (<50% luminal stenosis) and obstructive plaques (≥50% luminal stenosis). Two-vessel, 3-vessel, and left-main CAD were defined as multivessel disease. Each plaque was classified as follows: 1) noncalcified plaque = plaques having lower density compared with the contrast-enhanced vessel lumen without any calcification (>150 HU); 2) calcified plaque = plaque with predominantly calcification; or 3) mixed plaque = plaque with noncalcified having small amounts of calcified elements within a single plaque (6). Each plaque was also analyzed for the existence or absence of the following 3 features: low-attenuation plaque (LAP), positive remodeling (PR), and napkin-ring sign. First, noncalcified plaques were divided into LAP (plaque with <30 HU) or intermediate-attenuation plaques (plaque between 30 and 150 HU) (12,24). To identify the presence of LAP, a region of interest was placed on at least 5 randomly selected points within each plaque, and the mean value was defined as the plaque density. Second, manual inspection was used to define the remodeling index in both the axial and longitudinal reconstructions. The remodeling index was defined as the ratio of the vessel diameter at the plaque site to a reference diameter proximal to the lesion in a normal-appearing vessel segment. The presence of PR was defined by a remodeling index >1.1 (25,26). Finally, a napkin-ring sign was characterized by a plaque core with low computed tomography attenuation surrounded by a rimlike area of higher attenuation. More specifically, the napkin-ring sign was defined by the following criteria: 1) the presence of a ring of high attenuation around certain coronary artery plaques; and 2) attenuation of the ring, presenting higher than those of the adjacent plaque and not >130 HU. Representative cases of a napkin-ring sign are shown in Figure 1.

Endpoints. The pre-specified endpoints of this study were the occurrence of cardiac death or an ACS event. ACS events included nonfatal myocardial infarction, as defined by the European Society

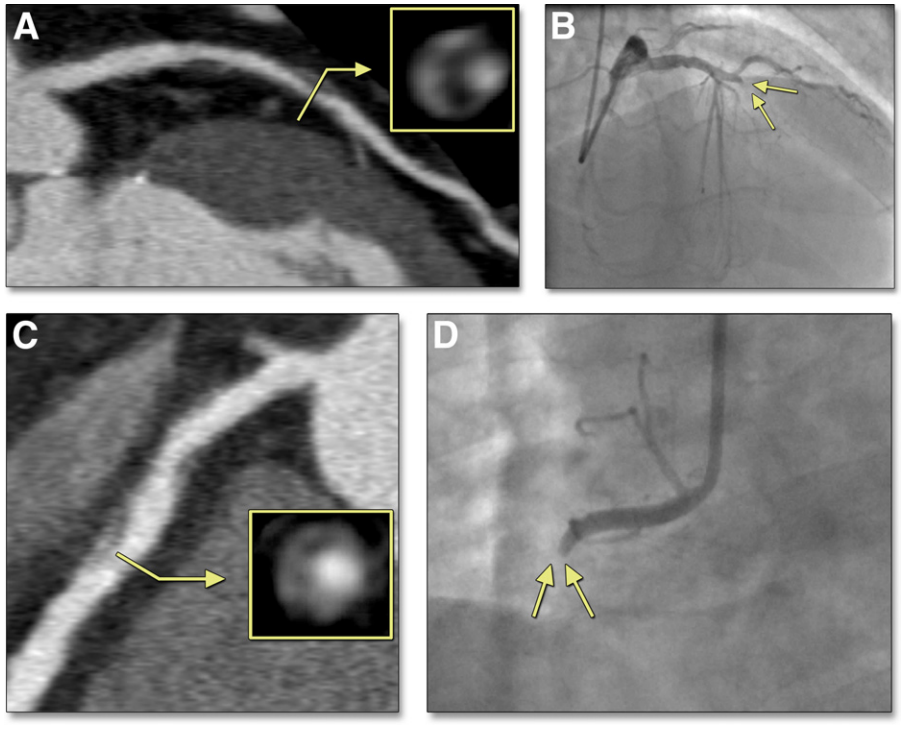

Figure 1. Representative Coronary CTA Images With Napkin-Ring Signs and Invasive Angiographic Images

(A) An atherosclerotic plaque with PR, LAP, and a napkin-ring sign in the proximal left anterior descending artery on coronary CTA. **(B)** Total occlusion of the proximal left anterior descending artery, causing acute myocardial infarction, by invasive coronary angiography 10 months after coronary CTA **(arrows)**. **(C and D)** coronary CTA images show an atherosclerotic plaque with PR, LAP, and a napkin-ring sign in the proximal right coronary artery, which was completely occluded 1 year later **(arrows)**. The **boxed area in A and C** indicates cross-sectional images of atherosclerotic plaque showing a napkin-ring sign. CTA = computed tomography angiography; LAP = low-attenuation plaque; PR = positive remodeling.

of Cardiology/American College of Cardiology Committee, and unstable angina, as defined according to the Braunwald classification (27,28). An ACS culprit lesion was determined based on the association of invasive coronary angiography with electrocardiographic changes, echocardiography, or myocardial ischemia as detected during a stress test.

Statistical analysis. Categorical variables are presented as number (%) and continuous variables as mean ± SD. The chi-square test was used for comparison of categorical variables. Between-group comparisons were made using either the independent-samples *t* test or the Mann-Whitney *U* test as appropriate. Cox proportional hazard analysis was performed to identify predictors of ACS events on per-segment and per-patient bases, respectively. Baseline variables that were considered clinically relevant or that showed a univariate relationship with outcome were entered into the analysis. The Kaplan-Meier survival method was used to compare survival rates according to existence or absence of a napkin-ring sign on coronary CTA, using the log-rank test. A p value <0.05 was considered statistically significant. Statistical analyses were performed with use of SPSS version 12.5 software (SPSS Japan Inc., Tokyo, Japan).

Interobserver variability of coronary CTA analysis was obtained by analysis of 50 random segments by 2 independent blinded observers. Intraobserver variability was determined by the analysis of the other 50 segments by the same observer at 2 different time points. A kappa test was used for interobserver and intraobserver variability of coronary CTA measurements.

RESULTS

Patient-based analysis of clinical characteristics associated with ACS. Survival was examined after a mean follow-up of 2.3 ± 0.8 years ranging from 1 year to 4.2 years (median 3.0 years), at which point 24 ACS events had occurred (2.7%; 11 per 1,000 population/year), comprising cardiac death in 1 patient, nonfatal myocardial infarction in 4 patients, and unstable angina in 19 patients. In 24 patients with ACS, all culprit lesions were confirmed by coronary angiography. Patients with ACS events had higher rates of hypercholesterolemia ($p = 0.02$), a history of myocardial infarction ($p < 0.001$), multivessel disease ($p < 0.001$), and higher serum C-reactive protein levels ($p = 0.048$) than those without ACS events (Table 1). Cox proportional hazard analysis identified multivessel disease as an independent risk factor associated with ACS events (Table 2).

Coronary CTA findings. Of the 13,425 segments examined in the 895 subjects, 188 segments were excluded because of scheduled revascularization within 1 month and 175 segments were excluded because of previous revascularization. A further 335 segments were also excluded from analysis due to

Table 1. Patient Characteristics That Did or Did Not Develop Into ACS Events

	Overall (N = 895)	Patients With ACS Events (n = 24)	Patients Without ACS Events (n = 871)	p Value
Male	590 (66)	17 (70)	573 (65)	0.4
Age, yrs	66 ± 10	65 ± 12	66 ± 10	0.7
Hypertension	595 (66)	18 (75)	577 (66)	0.4
Hypercholesterolemia	491 (55)	18 (75)	473 (54)	0.02
Diabetes	436 (49)	12 (50)	424 (48)	0.7
Current smoking	324 (36)	11 (45)	313 (35)	0.3
Body mass index, kg/m^2	24.4 ± 3.5	23.4 ± 3.9	24.5 ± 3.4	0.2
Previous myocardial infarction	180 (20)	10 (41)	170 (19)	<0.001
Multivessel CAD	269 (30)	18 (78)	251 (28)	<0.001
Total cholesterol, mg/dl	193 ± 42	197 ± 30	192 ± 42	0.7
LDL cholesterol, mg/dl	112 ± 35	124 ± 28	112 ± 35	0.2
HDL cholesterol, mg/dl	51 ± 14	48 ± 10	51 ± 14	0.6
Triglycerides, mg/dl	152 ± 107	133 ± 70	153 ± 108	0.4
Fasting glucose, mg/dl	126 ± 45	132 ± 39	126 ± 45	0.6
HbA_{1c}, %	5.8 ± 1.0	6.5 ± 1.3	5.8 ± 1.0	0.06
C-reactive protein, mg/l	1.0 ± 1.3	1.6 ± 1.3	1.0 ± 1.3	0.048
Framingham risk score	8.6 ± 3.9	9.3 ± 4.2	8.6 ± 3.8	0.4

Values are n (%) or mean ± SD.
ACS = acute coronary syndrome; CAD = coronary artery disease; HDL = high-density lipoprotein; LDL = low-density lipoprotein.

JACC: CARDIOVASCULAR IMAGING, VOL. 6, NO. 4, 2013
APRIL 2013:448–57

Table 2. Cox Proportional Hazard Analysis for the Development of Acute Coronary Syndrome Events on the Basis of Patient-Based Analysis

	Hazard Ratio (95% CI)	p Value
Hypercholesterolemia	2.13 (0.77–5.88)	0.1
Previous myocardial infarction	1.95 (0.83–4.54)	0.1
C-reactive protein, mg/l	4.69 (0.54–40.27)	0.1
Multivessel disease	7.19 (2.56–20.16)	<0.001

Adjusted for age, sex, hypertension, and diabetes.
CI = confidence interval.

the inadequate image quality, such as severe calcification and/or arrhythmia. Finally, 12,727 of the 13,425 segments (95%) were analyzed in this study. Of these, 1,174 contained plaques (average of 1.3 plaques per patient), including plaques with PR in 130 segments (1.0%), LAP in 107 segments (0.8%), and napkin-ring signs in 45 segments (0.4%). Napkin-ring signs were present concurrently with PR and LAP in 20 plaques (44%) and 30 plaques (67%), respectively. Thirty-six of 45 plaques (80%) with napkin-ring signs overlapped with those showing either PR or LAP. Fourteen plaques (33%) with napkin-ring signs had both PR and LAP. Coronary artery distributions of the napkin-ring sign were 9 (20%) in the right coronary artery, 3 (6.6%) in the left main coronary artery, 18 (40%) in the left anterior descending coronary artery, and 5 (11%) in the left circumflex coronary artery (Fig. 2). Most plaques with napkin-ring signs clustered in the proximal sites of vessels.

Segment-based analysis of coronary CTA findings associated with ACS. Ten culprit lesions (41%) occurred at the segment with napkin-ring signs on coronary CTA (0.1 ACS events per plaque with napkin-ring sign per year). Lesions resulting in ACS had an increased prevalence of obstructive plaques ($p < 0.001$), PR ($p < 0.001$), LAP ($p < 0.001$), and napkin-ring sign ($p < 0.001$) than those not associated with ACS events (Table 3). Cox proportional hazard analysis confirmed that PR ($p < 0.001$), LAP ($p = 0.007$), and napkin-ring sign ($p < 0.001$) were significant predictors of ACS events (Table 4).

Plaques with these coronary CTA features were more likely to be associated with ACS events than those without such findings (Fig. 3). Kaplan-Meier curves for ACS events based on the presence of napkin-ring signs with PR, LAP, and 3 high-risk features are shown in Figure 4. The presence of the napkin-ring sign yielded a sensitivity of 42%, a

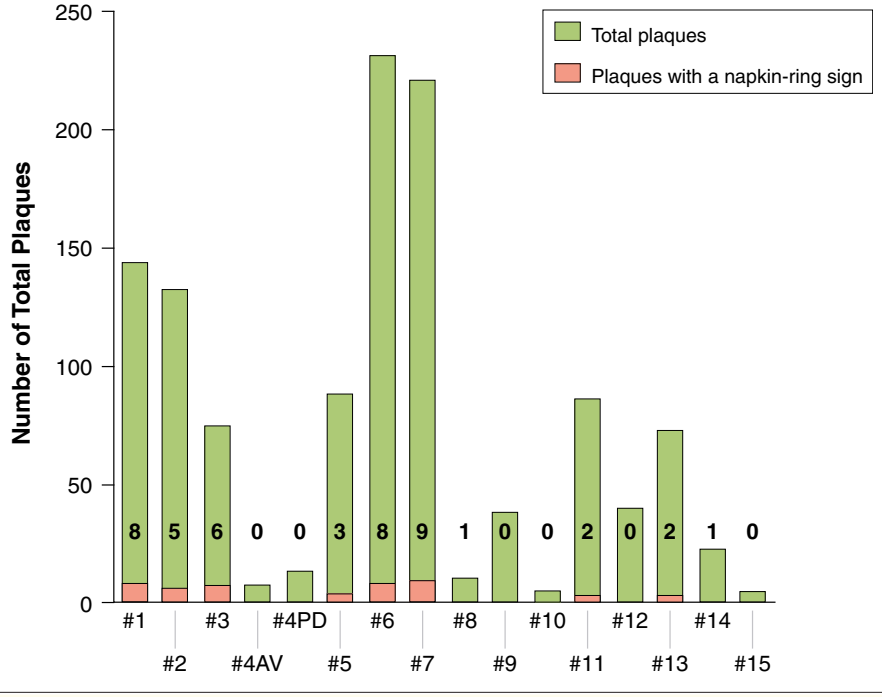

Figure 2. Distribution of Napkin-Ring Signs in Coronary Artery Trees

Forty percent of the napkin-ring signs was present in the left anterior descending coronary artery. Most plaques with napkin-ring signs clustered in the proximal sites of vessels.

Table 3. Segment-Based Comparison of Coronary Computed Tomography Angiography Characteristics With and Without ACS Events

	ACS Segments (n = 24)	No ACS Segments (n = 1,150)	p Value
Noncalcified plaque	11 (45)	409 (35)	0.3
Calcified plaque	1 (4.0)	132 (11)	0.3
Mixed plaque	12 (50)	608 (52)	0.8
Obstructive plaque	17 (70)	467 (42)	<0.001
Positive remodeling	14 (58)	116 (10)	<0.001
Low-attenuation plaque	13 (54)	94 (8.0)	<0.001
Napkin-ring sign	10 (41)	35 (3.0)	<0.001

Values are n (%).
ACS = acute coronary syndrome.

specificity of 97%, a positive predictive value of 22%, and a negative predictive value of 99% for determining future ACS events.

Excellent correlation was observed in interobserver and intraobserver variability of coronary CTA measurements. Values were $\kappa = 0.93$ and $\kappa = 1.0$ for plaque type, $\kappa = 0.92$ and $\kappa = 0.96$ for stenosis severity, $\kappa = 0.88$ and $\kappa = 0.91$ for positive remodeling, $\kappa = 0.83$ and $\kappa = 0.88$ for LAP, and $\kappa = 1.0$ and $\kappa = 1.0$ for the napkin-ring sign, respectively.

DISCUSSION

Napkin-ring sign on coronary CTA and ACS events. The recently developed modality of coronary CTA is a noninvasive and accurate technique for visual assessment of the degree of vessel luminal narrowing (5–9) and characterization of coronary atherosclerosis (10–15). The napkin-ring sign is one of the coronary CTA-based vulnerable coronary plaque morphologies, characterized by a plaque core with low attenuation surrounded by a rimlike area of higher attenuation, potentially representing TCFA (16–21). A recent dual-source coronary CTA study demonstrated a higher prevalence of napkin-ring signs among patients experiencing

Table 4. Cox Proportional Hazard Analysis for the Development of Acute Coronary Syndrome Events on the Basis of Segment-Based Analysis

	Hazard Ratio (95% CI)	p Value
Obstructive plaque	1.62 (0.63–4.17)	0.3
Positive remodeling	5.25 (2.17–12.69)	<0.001
Low-attenuation plaque	3.75 (1.43–9.79)	0.007
Napkin-ring sign	5.55 (2.10–14.70)	<0.001

CI = confidence interval.

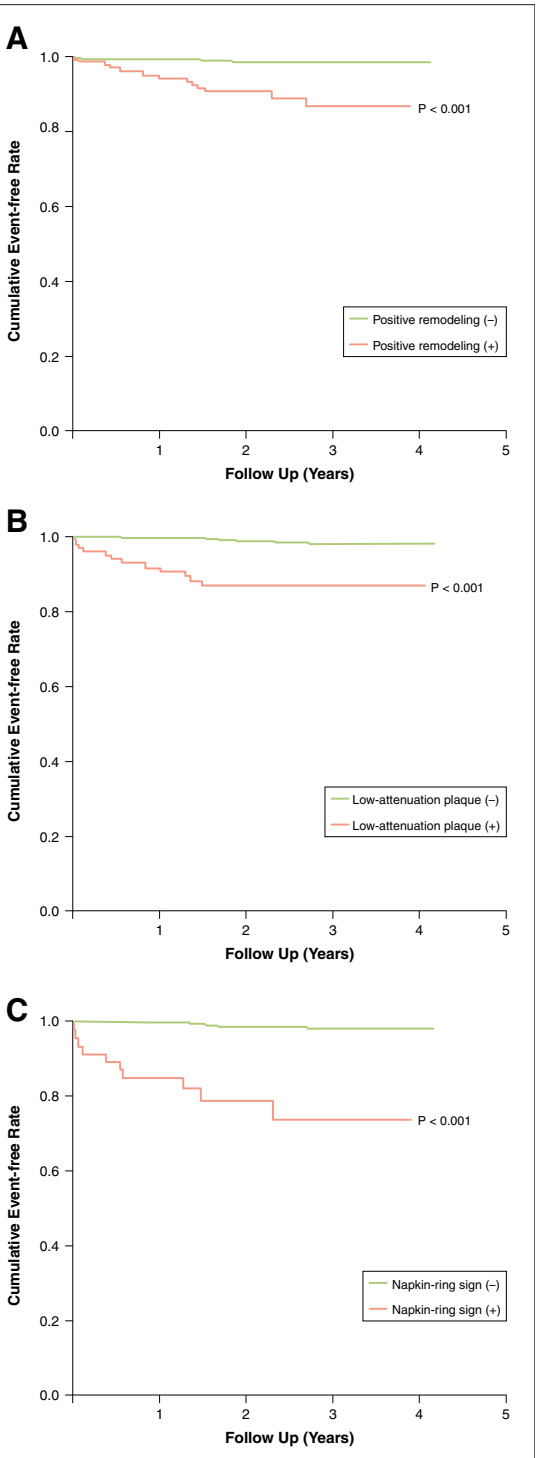

Figure 3. Kaplan-Meier Curves for ACS Events With or Without Each High-Risk CTA Feature

Event-free curves for acute coronary syndrome (ACS) events resulting from plaques with or without positive remodeling (**A**), low-attenuation plaque (**B**), and napkin-ring sign (**C**), respectively. Plaques with these high-risk coronary computed tomography angiography (CTA) features had a higher incidence of acute coronary syndrome events than those without such findings.

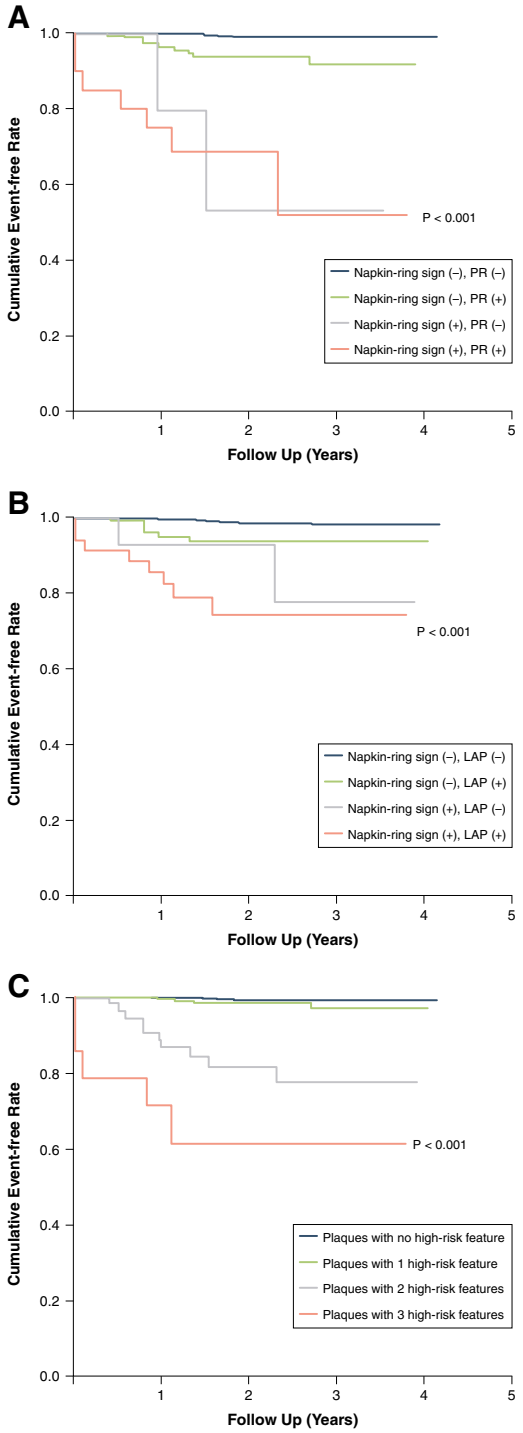

Figure 4. Kaplan-Meier Curves for ACS Events for Combination of 3 High-Risk Features

Event-free curves for acute coronary syndrome (ACS) events on the basis of the presence of the napkin-ring sign with positive remodeling (PR) **(A)** and low-attenuation plaque (LAP) **(B)**, and 3 high-risk features **(C)**, respectively. The presence of napkin-ring signs had an independent and additive prognostic impact on ACS outcome.

ACS events than among those with stable angina (29). Our previous investigation demonstrated a close relationship between the napkin-ring sign finding on coronary CTA and ruptured plaques on intravascular ultrasound (16). This finding was supported by similar studies comparing coronary CTA with optical coherence tomography (18,30) and coronary angioscopy (21). However, the prognostic role of the napkin-ring sign on future ACS events has not been investigated.

This study demonstrated for the first time that the finding of a napkin-ring sign on coronary CTA was of significant prognostic importance for ACS events as a surrogate marker of precursor lesions for rupture and thrombosis, independent of other coronary CTA features including PR and LAP. It may be explained by the possible mechanisms of the napkin-ring sign. They include intraplaque vasa vasorum enhancement by the coronary CTA contrast media, intraplaque hemorrhage or thrombus with peripheral enhancement by contrast media, or microcalcifications in the plaque, all of which are strongly associated with the presence of TCFA and future ACS development (18,19,25). Therefore, detection of the napkin-ring sign on coronary CTA could add specificity to the coronary CTA assessment of vulnerable plaques.

Prevalence and outcomes of vulnerable plaque. A number of pathological studies have proposed that disruption of TCFA may be a main cause of ACS events (4,31). Recent clinical investigations support this scenario, suggesting the capabilities of intracoronary imaging modalities to identify high-risk plaque developing into ACS events (32–34). However, no direct evidence has been postulated due to the lack of appropriate in vivo imaging modalities. Considering its noninvasive nature and ability to visualize the whole coronary artery, coronary CTA may provide the mechanical insight into the relationship between vulnerable plaques and future ACS events.

The napkin-ring sign and high-risk plaque on coronary CTA were observed in only 4.0% of the total plaques, which was similar to the prevalence of ruptured plaque or TCFA in an earlier postmortem study (2.7%) (31). In contrast, 6.5% to 19% of plaques were classified as high-risk plaques in invasive intravascular ultrasound investigations (32–34). This discrepancy may be due to underlying differences in atherosclerotic risks between these study populations. Consistently, the incidence rates of ACS events in our (2.7%; 11 per 1,000 population/year) and other coronary CTA (1.4%; 6.2 per 1,000

population/year to 4.2%; 13 per 1,000 population/year) studies (9,25,35,36) have been lower than in intravascular ultrasound investigations (8.6%; 34 per 1,000 population/year to 11%; 58 per 1,000 population/year) (32–34).

Surprisingly, 41% of ACS events occurred from plaques with napkin-ring signs (0.1 ACS event per napkin-ring plaque/year), which was higher than the results of intravascular ultrasound investigations (0.01 to 0.04 ACS event per high-risk plaque/year) (33,34). Therefore, the napkin-ring sign was superior to other features of high-risk plaque as representative of TCFA or a rupture-prone plaque in the near future. It has been reported that a stable fibrous plaque without necrosis could be falsely defined as vulnerable by intravascular ultrasound due to its spatial resolution (37). Of note, plaque characteristics are the determinants of the subsequent progression of atherosclerotic plaque, independent of systemic, traditional risk factors (38). Therefore, in addition to optimizing therapy based on systemic atherosclerotic risk factors, a more detailed risk stratification based on plaque characteristics is required to improve clinical outcomes.

Study limitations. First, this was a single-center study, and large-scale multicenter studies are needed to confirm our findings. Second, there was no volumetric quantification of plaque performed in this study, although the napkin-ring sign may be associated with the circumferential extent of a necrotic core in vulnerable plaques, so LAP volume may provide mechanical insight into the napkin-ring sign found on coronary CTA (20). Further, because the napkin-ring sign is considered a feature of vulnerable coronary plaque morphologies, it might not be associated with severe calcifications (19,20). However, 335 segments (3%) were excluded owing to heavy calcification or motion artifacts, and this may have caused a potential bias in this study. A third limitation is the concern of radiation exposure with coronary CTA. To make this modality a viable diagnostic tool, the radiation dose must be reduced. The relatively low sensitivity of the napkin-ring sign in predicting ACS events may limit the clinical use of coronary CTA. Several techniques, such as dose modulation, prospective triggering, and imaging with reduced tube voltage (100 kV) could decrease the radiation dose and potentially allow more widespread use of coronary CTA (29,39). Future studies are necessary to investigate whether these techniques would affect the HU values of soft tissues and the detection of napkin-ring signs. Finally, because of the limited spatial resolution of current coronary CTA systems, the detailed histopathological features of napkin-ring signs remain unclear (19). Adding noncontrast-enhanced coronary CTA, or multiple imaging modalities, such as intravascular ultrasound, optical coherence tomography, and coronary angioscopy, may provide further insight into the relationship between napkin-ring signs and TCFA (19,40).

CONCLUSIONS

This was the first study to demonstrate that napkin-ring signs on coronary CTA were closely associated with future ACS events, independent of the presence of PR and LAP. Detection of a napkin-ring sign could help identify patients at high risk of future ACS events.

Acknowledgments

The authors appreciate the assistance of many colleagues in the recordings and management of coronary CTA datasets and patient records: Makoto Sakamoto, MT, Chihiro Kakoiyama, RN, and Tomomi Watanabe, RN, (Osaka Ekisaikai Hospital); and Shigenori Sassa, MD (Sassa Medical Clinic).

Reprint requests and correspondence: Dr. Shota Fukuda, Department of Medicine, Osaka Ekisaikai Hospital, 2-1-10 Honden, Nishi-ku, Osaka 550-0022, Japan. *E-mail: h-syouta@mve.biglobe.ne.jp*.

REFERENCES

1. Falk E. Plaque rupture with severe pre-existing stenosis precipitating coronary thrombosis. Characteristics of coronary atherosclerotic plaques underlying fatal occlusive thrombi. Br Heart J 1983;50:127–34.
2. Naghavi M, Libby P, Falk E, et al. From vulnerable plaque to vulnerable patient: a call for new definitions and risk assessment strategies: part I. Circulation 2003;108:1664–72.
3. Tanaka A, Kawarabayashi T, Nishibori Y, et al. No-reflow phenomenon and lesion morphology in patients with acute myocardial infarction. Circulation 2002;105:2148–52.
4. Virmani R, Burke AP, Farb A, Kolodgie FD. Pathology of the vulnerable plaque. J Am Coll Cardiol 2006;47:C13–8.
5. Achenbach S, Ropers D, Hoffmann U, et al. Assessment of coronary remodeling in stenotic and nonstenotic coronary atherosclerotic lesions by multidetector spiral computed tomography. J Am Coll Cardiol 2004;43:842–7.
6. Pundziute G, Schuijf JD, Jukema JW, et al. Prognostic value of multislice computed tomography coronary angiography in patients with known or suspected coronary artery disease. J Am Coll Cardiol 2007;49:62–70.
7. Budoff MJ, Dowe D, Jollis JG, et al. Diagnostic performance of 64-multidetector row coronary computed tomographic angiography for evaluation of

coronary artery stenosis in individuals without known coronary artery disease: results from the prospective multicenter ACCURACY (Assessment by Coronary Computed Tomographic Angiography of Individuals Undergoing Invasive Coronary Angiography) trial. J Am Coll Cardiol 2008;52:1724–32.

8. Miller JM, Rochitte CE, Dewey M, et al. Diagnostic performance of coronary angiography by 64-row CT. N Engl J Med 2008;359:2324–36.
9. Gopal A, Nasir K, Ahmadi N, et al. Cardiac computed tomographic angiography in an outpatient setting: an analysis of clinical outcomes over a 40-month period. J Cardiovasc Comput Tomogr 2009;3:90–5.
10. Leber AW, Knez A, Becker A, et al. Accuracy of multidetector spiral computed tomography in identifying and differentiating the composition of coronary atherosclerotic plaques: a comparative study with intracoronary ultrasound. J Am Coll Cardiol 2004;43:1241–7.
11. Schroeder S, Kopp AF, Baumbach A, et al. Noninvasive detection and evaluation of atherosclerotic coronary plaques with multislice computed tomography. J Am Coll Cardiol 2001;37:1430–5.
12. Motoyama S, Kondo T, Anno H, et al. Atherosclerotic plaque characterization by 0.5-mm-slice multislice computed tomographic imaging. Circ J 2007;71:363–6.
13. Voros S, Rinehart S, Qian Z, et al. Coronary atherosclerosis imaging by coronary CT angiography: current status, correlation with intravascular interrogation and meta-analysis. J Am Coll Cardiol Img 2011;4:537–48.
14. Voros S, Rinehart S, Qian Z, et al. Prospective validation of standardized, 3-dimensional, quantitative coronary computed tomographic plaque measurements using radiofrequency backscatter intravascular ultrasound as reference standard in intermediate coronary arterial lesions: results from the ATLANTA (assessment of tissue characteristics, lesion morphology, and hemodynamics by angiography with fractional flow reserve, intravascular ultrasound and virtual histology, and noninvasive computed tomography in atherosclerotic plaques) I study. J Am Coll Cardiol Intv 2011;4:198–208.
15. Nakanishi K, Fukuda S, Shimada K, et al. Non-obstructive low attenuation coronary plaque predicts three-year acute coronary syndrome events in patients with hypertension: multidetector computed tomographic study. J Cardiol 2012;59:167–75.
16. Tanaka A, Shimada K, Yoshida K, et al. Non-invasive assessment of plaque rupture by 64-slice multidetector computed tomography–comparison with intravascular ultrasound. Circ J 2008;72:1276–81.
17. Nakazawa G, Tanabe K, Onuma Y, et al. Efficacy of culprit plaque assessment by 64-slice multidetector computed tomography to predict transient no-reflow phenomenon during percutaneous coronary intervention. Am Heart J 2008;155:1150–7.
18. Kashiwagi M, Tanaka A, Kitabata H, et al. Feasibility of noninvasive assessment of thin-cap fibroatheroma by multidetector computed tomography. J Am Coll Cardiol Img 2009;2:1412–9.
19. Maurovich-Horvat P, Hoffmann U, Vorpahl M, Nakano M, Virmani R, Alkadhi H. The napkin-ring sign: CT signature of high-risk coronary plaques? J Am Coll Cardiol Img 2009;3:440–4.
20. Narula J, Achenbach S. Napkin-ring necrotic cores: defining circumferential extent of necrotic cores in unstable plaques. J Am Coll Cardiol Img 2009;2:1436–8.
21. Nishio M, Ueda Y, Matsuo K, et al. Detection of disrupted plaques by coronary CT: comparison with angioscopy. Heart 2011;97:1397–402.
22. Budoff MJ, Cohen MC, Garcia MJ, et al. ACCF/AHA clinical competence statement on cardiac imaging with computed tomography and magnetic resonance. J Am Coll Cardiol 2005;46:383–402.
23. Austen WG, Edwards JE, Frye RL, et al. A reporting system on patients evaluated for coronary artery disease. Report of the Ad Hoc Committee for Grading of Coronary Artery Disease, Council on Cardiovascular Surgery, American Heart Association. Circulation 1975;51:5–40.
24. Marwan M, Taher MA, El Meniawy K, et al. In vivo CT detection of lipid-rich coronary artery atherosclerotic plaques using quantitative histogram analysis: a head to head comparison with IVUS. Atherosclerosis 2011;215:110–5.
25. Motoyama S, Sarai M, Harigaya H, et al. Computed tomographic angiography characteristics of atherosclerotic plaques subsequently resulting in acute coronary syndrome. J Am Coll Cardiol 2009;54:49–57.
26. Ozaki Y, Okumura M, Ismail TF, et al. Coronary CT angiographic characteristics of culprit lesions in acute coronary syndromes not related to plaque rupture as defined by optical coherence tomography and angioscopy. Eur Heart J 2011;32:2814–23.
27. Braunwald E, Antman EM, Beasley JW, et al. ACC/AHA 2002 guideline update for the management of patients with unstable angina and non-ST-segment elevation myocardial infarction—summary article: a report of the American College of Cardiology/American Heart Association task force on practice guidelines (Committee on the Management of Patients With Unstable Angina). J Am Coll Cardiol 2002;40:1366–74.
28. Antman EM, Anbe DT, Armstrong PW, et al. ACC/AHA guidelines for the management of patients with ST-elevation myocardial infarction—executive summary. A report of the American College of Cardiology/American Heart Association Task Force on Practice Guidelines (Writing Committee to revise the 1999 guidelines for the management of patients with acute myocardial infarction). J Am Coll Cardiol 2004;44:671–719.
29. Pflederer T, Marwan M, Schepis T, et al. Characterization of culprit lesions in acute coronary syndromes using coronary dual-source CT angiography. Atherosclerosis 2010;211:437–44.
30. Ito T, Terashima M, Kaneda H, et al. Comparison of in vivo assessment of vulnerable plaque by 64-slice multislice computed tomography versus optical coherence tomography. Am J Cardiol 2011;107:1270–7.
31. Cheruvu PK, Finn AV, Gardner C, et al. Frequency and distribution of thin-cap fibroatheroma and ruptured plaques in human coronary arteries: a pathologic study. J Am Coll Cardiol 2007;50:940–9.
32. Sano K, Kawasaki M, Ishihara Y, et al. Assessment of vulnerable plaques causing acute coronary syndrome using integrated backscatter intravascular ultrasound. J Am Coll Cardiol 2006;47:734–41.
33. Calvert PA, Obaid DR, O'Sullivan M, et al. Association between IVUS findings and adverse outcomes in patients with coronary artery disease: the VIVA (VH-IVUS in Vulnerable Atherosclerosis) Study. J Am Coll Cardiol Img 2011;4:894–901.
34. Stone GW, Maehara A, Lansky AJ, et al. A prospective natural-history study of coronary atherosclerosis. N Engl J Med 2011;364:226–35.
35. Carrigan TP, Nair D, Schoenhagen P, et al. Prognostic utility of 64-slice computed tomography in patients with suspected but no documented coronary artery disease. Eur Heart J 2009;30:362–71.

36. Aldrovandi A, Maffei E, Palumbo A, et al. Prognostic value of computed tomography coronary angiography in patients with suspected coronary artery disease: a 24-month follow-up study. Eur Radiol 2009;19:1653–60.
37. Thim T, Hagensen MK, Wallace-Bradley D, et al. Unreliable assessment of necrotic core by virtual histology intravascular ultrasound in porcine coronary artery disease. Circ Cardiovasc Imaging 2010;3:384–91.
38. Uemura S, Ishigami K, Soeda T, et al. Thin-cap fibroatheroma and microchannel findings in optical coherence tomography correlate with subsequent progression of coronary atheromatous plaques. Eur Heart J 2011;33:78–85.
39. Gilbert L, Raff M, Kavitha M, et al. Radiation dose from cardiac computed tomography before and after implementation of radiation dose–reduction techniques. JAMA 2009; 301:2340–8.
40. Tanaka A, Imanishi T, Kitabata H, et al. Morphology of exertion-triggered plaque rupture in patients with acute coronary syndrome: an optical coherence tomography study. Circulation 2008;118:2368–73.

Key Words: acute coronary syndrome ■ coronary CT angiography ■ prognosis.